Different sol-gel preparations of iron-doped TiO_2 nanoparticles: characterization, photocatalytic activity and toxicological analysis.

V. Caratto[a], F. Locardi[b]*, S. Alberti[b], E. Sanguineti[a], A. Martinelli[c], R. Fabbri [a,] T. Balbi [a], Laura Canesi [a] , M. Ferretti[b].

a Department of Earth, Environmental and Life Sciences, University of Genoa, Corso Europa 26, 16132 Genova, Italy
b Department of Chemistry and Industrial Chemistry, University of Genoa, via Dodecaneso 31, 16146 Genova, Italy.

[C] CNR-SPIN, Corso Perrone 24, 16152 Genova

*Corresponding author email address: federico.locardi@unige.it

Abstract:

Fe-doped TiO_2 were prepared by sol-gel method using titanium tetraisopropoxide as the precursor of titania, 2-propanol as solvent, iron(III) chloride as dopant source through calcination at 350°C. Three different experiments were performed. The samples were characterized by means of X-ray powder diffraction (XRD), diffuse reflectance spectroscopy (DRS), scanning electron microscopy (SEM), Brunauer–Emmett–Teller analysis (BET). Photocatalytic activity of Fe-doped TiO_2 powders was evaluated through methylene blue degradation experiments conducted under simulated solar light irradiation. To evaluate the cytotoxic potential of the nanoparticles, in vitro test have also been performed.

1. Introduction

Semiconductor oxides, as polycrystalline nanoparticles, e.g. TiO_2, are important catalysts and catalytic supports; furthermore they also have photocatalytic and sensing applications [Xiang 2014, Kapilashram 2014]. Photocatalysis is a phenomenon in which a substance, a photocatalyst, is able to change the speed of a chemical reaction through the action of the light. TiO_2 finds several applications as a photocatalyst, because of its peculiar optical and chemical properties: it can decontaminate water with medium/low pollutants concentrations (water treatment) [Sturini 2012]; it can photo-degrade nitrogen oxides, emitted from exhaust pipes, when applied to the road surface [?]; it possesses self-cleaning capability when used as a coating for surfaces, (advanced photochemical applications) [Ball 2014]; moreover it finds applications also for solar energy production [].
When TiO_2 is irradiated by light with wavelength equal to 387 nm, electrons are promoted across the band gap (3.2 and 3.0 eV in the anatase and rutile polymorphs, respectively [?]) into the conduction band, leaving holes in the valence band. These holes are highly oxidizing and react with the adsorbed hydroxide ions, inducing the formation of hydroxyl radicals; these radicals are the main oxidizing species responsible for the photooxidation of organic compounds. However, the application of undoped TiO_2 is limited, because it requires UV activation; in fact, only less than 5% of the solar radiation which reaches the surface of the earth can be used. Consequently, considerable effort has been directed toward expanding the optical response of TiO_2 from the UV to the visible light region or using innovative method to increase the general efficiency [Zang 2004], as described in our recent work [Locardi, 2016]. When doped with transition metals, lanthanides, or non-metals atoms (such as V, Fe, Zn, Eu or S, C and N) TiO_2 can extend its photocatalytic activity in the visible region [Lee 2013, Wang 2012, Nishijima 2007,

Wang 2015, Pelaez 2012, Jaimy 2011]. A common synthesis for the preparation of the doped-catalyst nanoparticles consists in the sol-gel method.
Several articles report the synthesis of Fe-doped TiO_2 nanoparticles, with the best iron molar percentage of 0.5, in order to shift the energy gap and consequently to improve the photocatalytic properties [Kokila, Zhou]. Even if the syntheses performed were similar, some differences can be underlined: Kokila *et al.* [] have used a conventional sol-gel method starting from titanium^{IV} isopropoxide, ferric chloride and ethanol as solvent. Zhou *et al.* [] have performed the synthesis using titanium tetrachloride, iron^{III} chloride with the addition of the hexadecyltrimethyl ammonium bromide (CTAB) as surfactant. On the contrary Wang *et al.* [] started from the tetrabutyl titanate.
Consequently the aim of this work is to compare the chemical-physical properties and photocatalytic activity of 0.5 Fe-doped nanoparticles synthesized by different sol gel method in order to evaluate the influence of the reagent ratio; moreover also the cytotoxic effect of the compounds prepared has been investigated.

2. Experimental Procedure

Several TiO_2 samples doped with 0.5% (molar ratio) of Fe^{3+} with sol-gel process have been synthesized.

3.1 Synthesis

Sample 1: Titanium tetraisopropoxide (Sigma Aldrich, 97%), 2-propanol (Sigma Aldrich 99,9%) and H2O have been mixed (7.8:16.7:1 V/V) and left, at room temperature, under vigorous stirring for 4 hours. Then a solution of $FeCl_3$ in 2-propanol (16 mg in 30 mL) has been added and the final mixture, always stirred, has been placed over a hotplate for 2 hours at 90°C and then placed in a oven for 12 hours at 100°C.
Sample 2: Titanium tetraisopropoxide (Sigma Aldrich, 97%), 2-propanol (Sigma Aldrich, 99,9%) have been mixed together (1:6, V/V). Then, a solution of $FeCl_3$ in 2-propanol and immediately after a solution of H2O and NH4OH 25% (V/V) have been added (6:1, V/V) and mixed together with the former solution. After 30 minutes of stirring, the temperature has been increased up to 90°C and kept for 4 hours under the fume hood. The final suspension has been put in a oven for 8 hours at 100°C.
Sample 3: According to our previous work, Caratto *et al* [],titanium isopropoxide, isopropanol and water have been used as precursors with the same concentrations reported changing the different solution of H_2O and NH_3 with an unique solution of 16 mg of $FeCl_3$ in 30 mL of water, corresponding to a solution with a concentration of 3,3 mM.

The synthesized samples from the different methods have been finally treated in a muffle furnace (Carbolite RHF1400) at 350°C for 1 hour.

The samples have been analyzed by X-ray diffraction (XRD), electron microscopy (SEM), diffuse reflectance spectroscopy, Brunauer–Emmett–Teller analysis (BET). Phase identification was performed by X-ray powder diffraction analysis using a Philips PW1830 diffractometer (Bragg–Brentano geometry; Cu Kα; Ni filtered; range 20–80 2θ; step 0.025 2θ; sampling time 10 s). By using XRD data, structural refinement and micro-structural analysis were carried out according to the Rietveld method, using the Fullprof program; refinements were carried out using a file describing the instrumental resolution function. Scanning electron microscopy (SEM) was performed using a Tescan Vega 3 XMV microscope on powders coated with gold in low vacuum. Diffuse reflectance spectroscopy was performed using a Perkin Elmer UV-Vis spectrophotometer LAMBDA 35 equipped with an integrating sphere. Brunauer–

Emmett–Teller (BET) analysis was carried out using an ASAP 2010 physisorption analyzer (Micromeritics Instrument Corp). Before to the measurement the samples were pre-treated at 200 °C in vacuum.

3.2 *Photocatalytic tests*

The photocatalytic activity was tested using 12.5 mg of catalyst in 25 mL of an aqueous methylene blue (MB) solution ($3.12 \cdot 10^{-5}$M). Before the irradiation the suspensions were kept in the darkness under magnetic stirring for 20 minutes to establish the adsorption-desorption equilibrium between the particles and the colorant. Therefore, the first sampling was took (t_0) and the solar spectrum lamp (300W Ultra-Vitalux, Osram) was turned on and maintained at 20 cm from the suspensions. The experiment was performed for a total of 50 minutes by sampling every 10 minutes. The collected samples were centrifuged (Centrifuge 5410, Eppendorf) at 13200 rpm for 5 minutes to separate the particles possibly present in suspension and then were analyzed by means of a UV-Vis spectrometer (Perkin Elmer Lambda 35) in the 200-800 nm range. The MB concentration was calculated monitoring the absorbance at 664 nm.

3.3 Cell culture and treatments

Human umbilical vein endothelial cells (HECV) were purchased from Interlab Cell Line Collection (ICLC, Genova, Italy). Cells were grown in Dulbecco's Modified Eagle's Medium (DMEM) (Euroclone, Milan, Italy) supplemented with 10% FCS (Euroclone, Milan, Italy) and cultured at 37°C in 5% CO_2 humid incubator. Cells were seeded in 96-well plates (104 cells/well) and incubated for 24 h at 37°C in 0.2 ml DMEM without Phenol Red (exposure medium) supplemented with 10% FCS. Cells were then incubated for 24 h with different concentrations of the three different types of Fe-doped TiO_2 nanoparticles (0.1-1-10 µg/ml) suitably diluted from a 1 mg/ml stock solution in exposure medium supplemented with 0.4% FCS and dispersed by bath sonication for 15 min. Controls samples were run in parallel. For each sample, four experiments were performed in six replicates.
Cell viability was evaluated by the 3-(4,5-dimethylthiazol-2-yl)-2,5-diphenyltetrazolium bromide (MTT) assay, based on the reduction of the soluble yellow tetrazolium salt MTT by the mitochondrial dehydrogenase of viable cells into a blue insoluble formazan product with an absorbance maximum near 570 nm [Mosmann, 1983]. Nitric oxide production was evaluated by measuring nitrite accumulation according to the Griess method [Green et al., 1982], and optical density was measured at 540 nm. Concentrations of nitric oxide in the samples were determined using a calibration curve generated with standard $NaNO_2$ solutions (0.1-100 µM). Readings were corrected for background absorbance of NM suspensions in exposure medium in the absence of cells.

3. Results and discussions

3.1 XRD Diffraction

The XRD patterns evidences that anatase is the main phase in all the three samples (Figure Alb1); moreover, it is also evident the presence of brookite, revealed by the weak 121 peak at Q ~ 2.15 $Å^{-1}$.
Rietveld refinements were hence carried out using a structural model foreseeing the coexistence of anatase with brookite (Fig. Alb2); the obtained results are reported in Table Alb1. The anatase lattice parameters are quite similar in sample 2 and 3, whereas the content of the secondary brookite is much larger for sample 3. The microstructural analysis reveals that the average size of the coherent diffraction domains (CDD; to be not confused with particle size) characterizing the anatase particles ranges around

5 nm, for all the three samples (Table Alb1). In all the samples the standard deviation from the average CDD size is close to 0, indicating that sizes are spread out over a narrow range of values. Remarkably, the refinement of the anisotropic size parameters reveals that the CDD are characterized by an almost spherical shape.

3.2 SEM analysis

The SEM micrographs of the three samples presented in Fig. X show different morphologies and distribution of the particles. In sample 1 (Fig X a) most of particles are agglomerated in elongated structure at the micrometric scale. Sample 2 (Fig X b) is characterized by the presence of nanosized particles, high homogeneity, almost spherical shape and tendency to form sponge-like aggregates. Sample 3 shows an agglomerated structure with a more porous surface than sample 1. The results prove that the synthesis method caused significant changes in the morphology of the obtained samples. These data is probably related to both the ratio of alkoxide/water and pH of the suspension. In fact only in sample 2 a solution of NH_4OH was added; the other samples were extremely acidic due to $FeCl_3$ solution

3.3 Photocatalytic activity

The photocatalytic activity of the synthesized samples has been investigated using the methylene blue as dye according to the ISO standard 10678:2010.
Despite the ISO standard, in literature it was found that the study of photo-degradation of Fe-doped TiO_2 on organic pollutants has been run on different chemicals, such as Methyl Orange, Acid Red Dye and Phenol. Kokila *et al.* [] measured the photocatalytic activity using a methylene orange solution. He reached, after 90 min, a degradation equal to 65%; the ration between the dye and the photocatalyst was set at 3.75g/L TiO_2-Fe / 0.003 g/L of methylene orange solution. Zhou et al. used the acid red dye, measuring an activity higher respect to the previous group, equal to the 77% after 60 min; for this test the ratio was set to 7.5 g/L TiO_2-Fe 0.05 g/L to ARD. In Figure XX the photocatalytic results obtained, using our three different compounds, have been presented; for this test the ratio was set to 0.5 g/L TiO_2-Fe 0.01 g/L to MB . As shown, after 50 minutes of solar-simulated light treatment, sample 1 reaches a degradation of 43±3,3%), which results rather lower than sample 2 and 3, which reach the values of, respectively, 77±2.5% and 75% ±3%. Moreover, assuming that the kinetics of reaction follow a first order law, the corresponding value of the kinetic constant is, for sample 1, 0.0114 sec^{-1} while for sample 2 and sample 3, is respectively of 0.0298 sec^{-1} and 0.0286 sec^{-1}. The diffuse reflectance analyses have revealed a similar red shift in the adsorbing spectra; in particular the absorbance changed from 377 nm for the undoped sample [], to 384 – 384.8 – 383 nm respectively for the samples 1, 2 and 3. The modification of the spectra is reflected also in the energy gap which result 3.29 eV for the pure TiO_2 and 3.22 – 3.22 – 3.23 eV for the three samples. As expected, being the compounds doped with the same amount of iron, a possible modification in the adsorbing spectrum could be correlated only in different particle dimensions; but how the XRD refinement has shown, the crystallites were the same for all the three compounds. In fact, it is documented that the changes in the energy gap is strictly correlated to the crystallite dimensions. Indeed, the significant lower photoactivity of the sample 1 is correlated to a very low surface area; in fact the BET analysis has revealed a value of only 16.73 m^2/g significant lower respect to the sample 2, 106.15 m^2/g and to the sample 3, 112.93 m^2/g. The BET analyses are consistent with the SEM images that reveal how the sample 1, respect to the other, is formed by huge agglomerates with a ceramic aspect. Consequently it can be assumed that the quantity of Titanium tetraisopropoxide, respect to the solvent (water and isopropanol) should be carefully checked; in fact the too low amount of solvent inhibits the correct formation of the gel inducing the agglomeration of the nanoparticles. In comparison to the results documented in literature, through the samples 2 and 3 , which we have

described, it was possible to obtain a better catalytic activity respect to Kokila *et al.* and Zang *et al.*, being the final degradation percentage equal or major using a lower catalytic amount.

3.4 Cell viability and NO production

In vitro tests were performed in order to evaluate the cytotoxic potential of the selected NPs in HECV cells. Sample 3 NPs induced a dose dependent decrease in cell viability, that was maximal (-40%; $p \leq 0.05$) at 10 µg/ml. On the other hand, exposure to samples 1 and 2 NPs induced a significant decrease in cell viability only at the highest concentration tested (10 µg/ml) (-20 and -40%, respectively; $p \leq 0.05$). Fig. XX

Sample 2 NPs induced a significant increase in NO production, with highest levels at the lowest concentration tested (0.1 µg/ml; $p \leq 0.01$). Such an induction was not observed at 10 µg/ml, where a significant decrease in the cell viability was obtained. No changes were observed with sample 1 and 3 NPs.

The strong toxicity of sample 3 can be correlated with its higher photoactivity, respect to the other samples, which is strictly correlated with a major surface area directly responsible in the formation of the free hydroxyl radicals. In fact, sample 1, which was resulted the low toxic, possesses the lower surface are being formed by particle agglomerates. Hence, we can affirm that the cytotoxicity and the photocatalytic activity are strictly correlated and dependent on the aggregation state and surface area.

4 Conclusions

The effect of the three different reagents ratio in the sol gel synthesis of iron doped TiO_2 nanoparticles has been studied. In all the studied cases, the samples are constituted of a main anatase phase plus about 25-30 wt% of brookite, The diffuse reflectance analyses did not reveal any difference in the adsorption spectra, a result consistent with the fact that the iron doping concentration was set to 0.5%mol for all the syntheses. On the contrary the reagents ratio influences the other properties such as the surface area, the aggregation state, the photoactivity and the cytotoxicity: when the Titanium tetraisopropoxide and the propanol has been set in the 1:2 ratio, the formation of particles agglomerates with low surface area, and consequently low photoactivity, occurred. Maintaining the same ratio but increasing by 5 times the H_2O volume, the nanoparticles decrease their dimension and increase the surface area and the degradation activity. Similar results have been obtained changing the ratio Titanium tetraisopropoxide/propanol in 1:12. Consequently a high solvent volume respect to the Titanium tetraisopropoxide concentration is needed to observe the formation of nanoparticles with high surface area without the formation of agglomerates. Finally the cytotoxicity of the samples synthesis has been evaluated and a correlation with the photocatalytic activity has been established.

References

L. Ball, V. Caratto, E. Sanguineti, I. Firpo, M. Ferretti, P. Pelosi, Antibacterial activity of TiO2 nanoparticle coated endotracheal tubes: an in vitro study on Pseudomonas aeruginosa and Staphylococcus aureus, Eur. J. Anaesth. 31 (2014) 77.

L.C. Green, D.A. Wagner, J. Glogowski, P.L. Skipper, J.S. Wishnok, S.R. Tannenbaum, Analysis of nitrate, nitrite and [15N]nitrate in biological fluids, Anal. Biochem. 126 (1982) 131-138.

M. Kapilashrami, Y. Zhang, Y.S. Liu, A. Hagfeldt, J. Guo, Probing the optical property and electronic structure of TiO_2 nanomaterials for renewable energy applications, Chem. Rev. 114 (2014) 9662-9707.

K. B. Jaimy, S. Ghosh, S. Sankar, K.G.K. Warrier, An aqueos sol-gel synthesis of chromium (III) doped mesoporous titanium dioxide for visible light photocatalysis, Mater. Res. Bull. 46 (2011) 914-921.

H.U. Lee, S.C. Lee, S. Choi, B. Son, H. Kim, S.M. Lee, H.J. Kim, J. Lee, Influence of visible-light irradiation on physicochemical and photocatalytic properties of nitrogen-doped three-dimensional (3D) titanium dioxide, J. Hazard. Mater. 258-259 (2013) 10-18.

F. Locardi, E. Sanguineti, M. Fasoli, M. Martini, G.A. Costa, M. Ferretti, V. Caratto, Photocatalytic activity of TiO2 nanopowders supported on a new persistent luminescence phosphor, Catal. Commun. 74 (2016) 24-27.

T. Mosmann, Rapid colorimetric assay for cellular growth and survival: Application to proliferation and cytotoxicity assay, J. Immunol. Methods 65 (1983) 55-63.

K. Nishijima, B. Ohtani, X. Yan, T. Kamai, T. Chyoya, T. Tsubota, N. Murakami, T. Ohno, Incident light dependence for photocatalytic degradation of acetaldehyde and acetic acid on S-doped and N-doped TiO_2 photocatalysts, Chem. Phys. 339 (2007) 64-72.

M. Pelaez, N. T. Nolan, S. C. Pillai, M. K. Seery, P. Falaras, A. G. Kontos, P. S.M. Dunlop, J. W.J. Hamiton, J. A. Byrne, K. O'Shea, M. H. Entezari, D. D. Dionysiou, A review on the visible light active titanium dioxide photocatalysts for environmental applications, Appl. Catal. B-Environ 125 (2012) 331-349.

M. Sturini, A. Speltini, F. Maraschi, A. Profumo, L. Pretali, E.A. Irastorza, E. Fasani, A. Albini, Photolytic and photocatalytic degradation of fluoroquinolones in untreated river water under natural sunlight, Appl. Catal. B-Environ. 119-120 (2012) 32-39.

S. Wang, J.S. Lian, W.T. Zheng, Q. Jiang, Photocatalytic property of Fe doped anatase and rutile TiO_2 nanocrystal particles prepared by sol–gel technique, Appl. Surf. Sci. 263 (2012) 260–265.

Q. Wang, G. Yun, N. An, Y. Shi, J. Fan, H. Huang, B. Su, The enhanced photocatalytic activity of Zn^{2+} doped TiO_2 for hydrogen generation under artificial sunlight irradiation prepared by sol-gel method, J. Sol-Gel Sci. Technol. 73 (2015) 341-349.

D. Xiang, F. Qu, X. Chen, Z. Yu, L. Cui, X. Zhang, J. Jiang, H. Lin, Synthesis of porous ZnO nanospheres for gas senser and photocatalysis, J. Sol-Gel Sci. Technol. 69 (2014) 370-377.

J. Zhang, F. Pan, W. Hao, Q. Ge, T. Wang, Light-storing photocatalyst, Appl. Phys. Lett. 85 (2004) 5778-5780

Figure Captions

Fig. 1: XRD patterns of the analyzed samples (normalized data); the 121 diffraction peak of brookite is arrowed.

Fig. 2: Rietveld refinements plots of the three samples. The points in the upper field represent the observed intensity data, the calculated pattern is superposed and drawn as a solid line; the small vertical bars indicate the position of the allowed Bragg reflections for anatase (upper bars) and brookite (lower bars); the difference between the observed and calculated patterns is plotted in the lower field.

Fig. 3: The SEM images (HV: 20.0 kV, magnification: 10.0 kx) show a comparison between sample 1 (a), sample 2 (b) and sample 3 (c).

Fig. 4: Degradation of methylene blue by the three different samples: 1, 2 and 3

Fig. 5: Dose dependent decrease in cell viability in samples 1, 2 and 3 and NO production in sample 2.

Table Caption

Table 1: Structural and microstructural data obtained after Rietveld refinement; in the CDD field the average coherent diffraction domain size for anatase is reported.

Figures

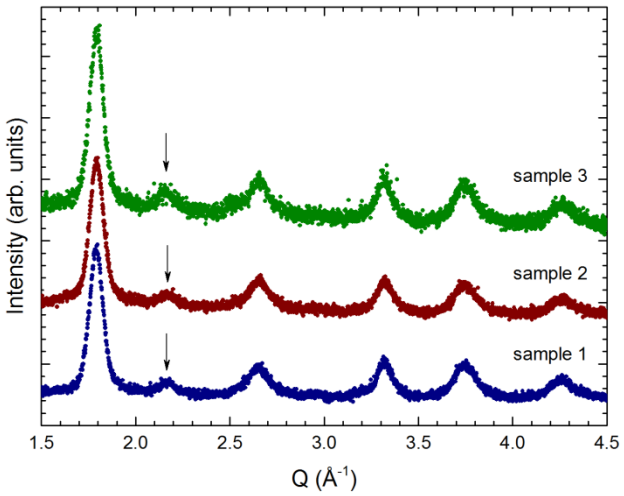

Fig. 1

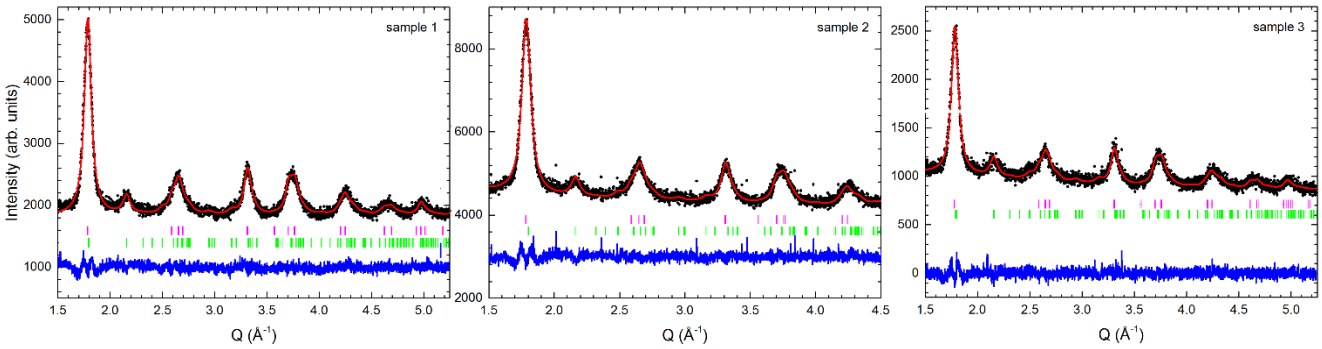

Fig. 2

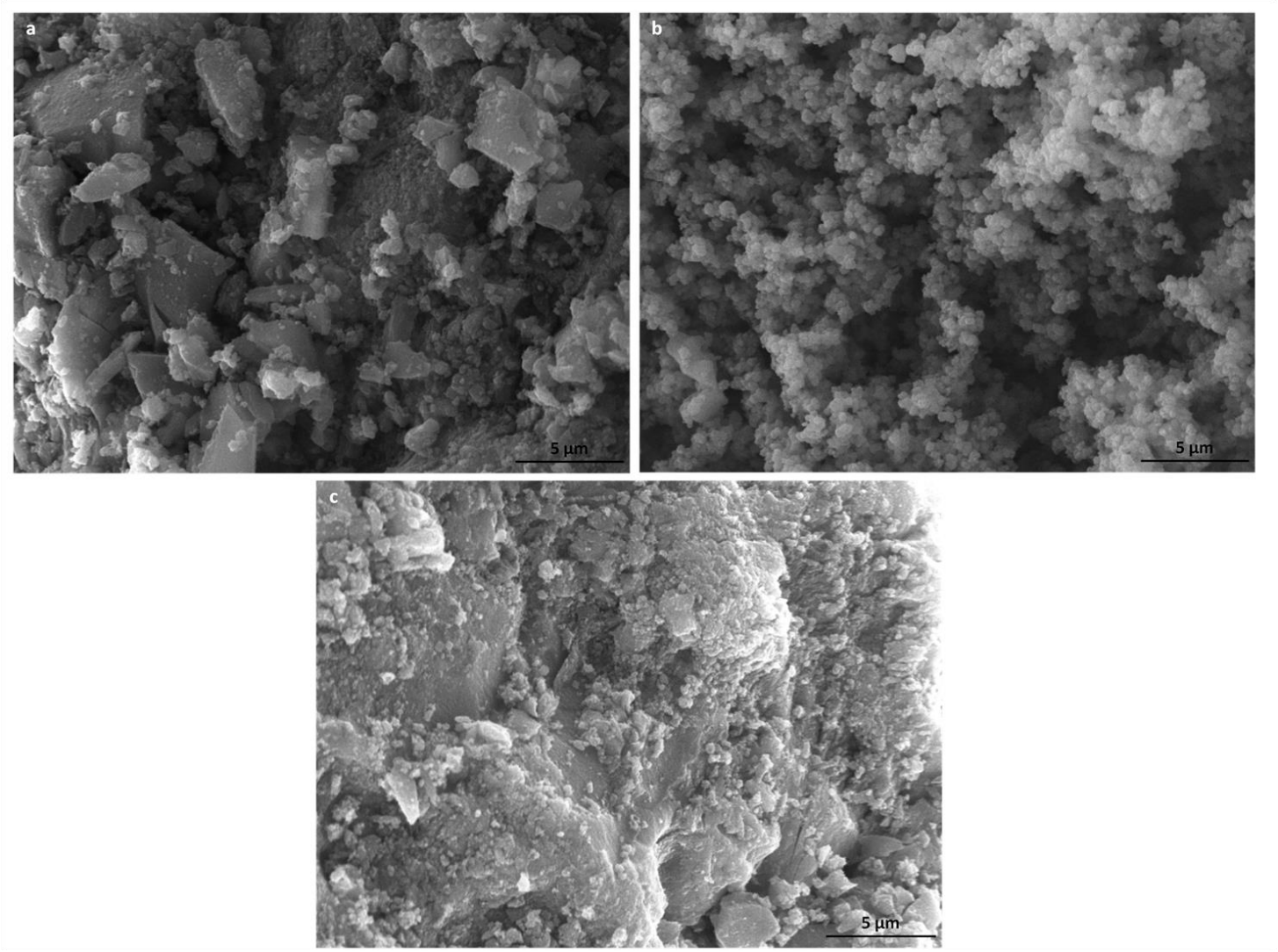

Fig 3

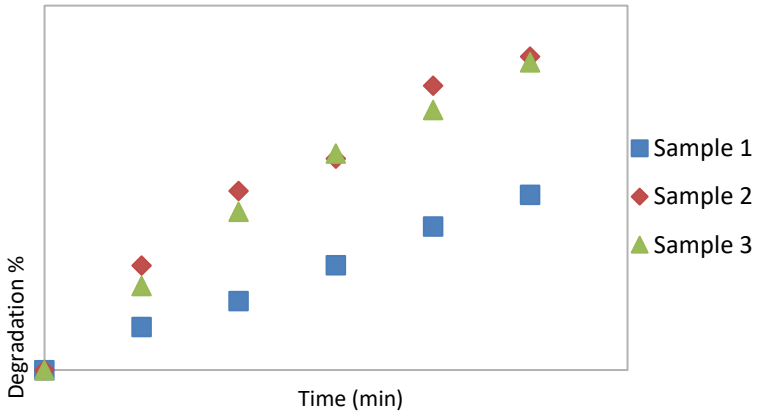
Degradation %
Time (min)
Sample 1
Sample 2
Sample 3

Fig. 4

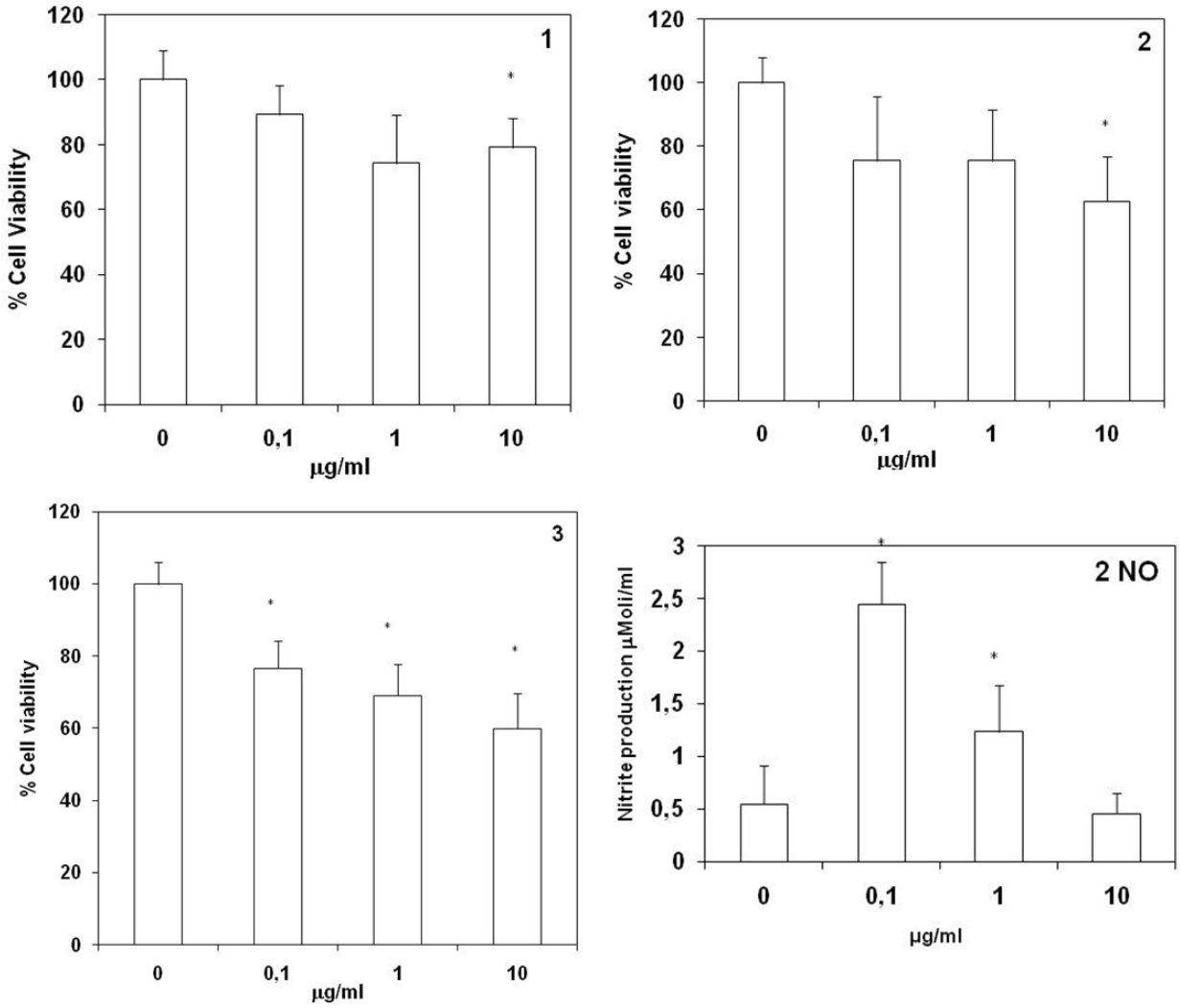
1
% Cell Viability
µg/ml
2
% Cell viability
µg/ml
3
% Cell viability
µg/ml
2 NO
Nitrite production µMoli/ml
µg/ml

Fig. 5

Tables

Table 1

	Sample 1	Sample 2	Sample 3
a (Å)	3.7946(1)	3.8002(1)	3.8026 (2)
c (Å)	9.4772(4)	9.4918(3)	9.4937(2)
Brookite (wt%)	26.5(1)	27.8(1)	35.5(2)
R_{wp} (%)	2.77	1.75	3.86
CDD size (nm)	4.9	5.4	4.9